Photoacoustics 28 (2022) 100403

Contents lists available at ScienceDirect

Photoacoustics

journal homepage: www.elsevier.com/locate/pacs

Dual-comb quartz-enhanced photoacoustic spectroscopy

Xinyi Ren [a], Ming Yan [a,b,*], Zhaoyang Wen [a], Hui Ma [a], Ran Li [a], Kun Huang [a,b], Heping Zeng [a,b,c,*]

[a] State Key Laboratory of Precision Spectroscopy, East China Normal University, Shanghai 200062, China
[b] Chongqing Key Laboratory of Precision Optics, Chongqing Institute of East China Normal University, Chongqing 401120, China
[c] Jinan Institute of Quantum Technology, Jinan, Shandong 250101, China

ARTICLE INFO

Keywords:
Photoacoustic
Optical frequency comb
Spectroscopy
Mid-infrared
Gas sensing

ABSTRACT

Photoacoustic spectroscopy (PAS) using two optical combs is a new-born technique, offering appealing features, including broad optical bandwidths, high resolutions, fast acquisition speeds, and wavelength-independent photoacoustic detection, for chemical sensing. However, its further application to, e.g., trace detection, is jeopardized due to the fundamentally and technically limited sensitivity and specificity. Here, we take a different route to comb-enabled PAS with acoustically enhanced sensitivity and nonlinear spectral hole-burning defined resolution. We demonstrate dual-comb quartz-enhanced PAS with two near-infrared electro-optic combs and a quartz tuning fork. Comb-line-resolved multiplexed spectra are acquired for acetylene with a single-pass detection limit at the parts-per-billion level. The technique is further extended to the mid-infrared (for methane), enabling improved sensitivity. More importantly, we measure nonlinear dual-comb photoacoustic spectra for the $^{12}C_2H_2$ $\nu_1 + \nu_3$ band P(17) transition with sub-Doppler pressure-broadening dominated homogeneous linewidths (e.g., 45.8 MHz), hence opening up new opportunities for Doppler-free photoacoustic gas sensing.

1. Introduction

Spectroscopic gas sensing has broad applications, ranging from trace detection to medical analysis [1,2]. Dual-comb spectroscopy (DCS) with photoacoustic (PA) detection (aka dual-comb PAS) [3,4] has recently brought new opportunities to these demanding applications. By harnessing two optical combs of slightly different line-spacings for scan-free Fourier-transform spectroscopy [5], DCS offers a unique solution for optimizing the trade-off among spectral resolutions, optical bandwidths, and measurement times, thus being advantageous in broadband molecular spectroscopy [6], transient chemical analysis [7] and high-resolution atmospheric sensing [8], and holding much promise for hyperspectral holography [9] and biomedical imaging [10]. Particularly, the multiplexing capacity of DCS, accompanied by the superior spectral resolving power (without the physical constraints) [5], allows molecular absorption lineshapes to be measured simultaneously on a comb line-by-line basis, benefiting accurate spectral analysis. PA detection of periodic thermal expansion pressure waves, induced by modulated light absorption of the molecules, with a sound transducer, dodges the limitations of direct photo-detection of light absorption regarding detector spectral responsivity, light background, and sample volume. Recent advancement in optical comb technology offers an unmatched light source [11], featuring evenly spaced narrow-linewidth comb lines in a super-broad spectrum (e.g., a single comb covering 3–27 μm) [12], hence being capable of interrogating almost any fundamental ro-vibrational lines of the molecules. However, despite the promising future, dual-comb PAS, a newborn technique, faces fundamental and technical challenges, preventing its application to, e.g., trace gas analysis. For instance, in the first demonstration [4], the sensitivity (at parts-per-million or ppm level) was limited by the microphone and the excitation of vibrational overtones. Also, the molecular spectra suffered from significant non-instrumental linewidth broadening, overshadowing the potential of DCS for Doppler-limited or even sub-Doppler measurements.

Intrinsically improving the spectral specificity calls for an effective means of differentiating inhomogeneously broadened and blended molecular lines. Nonlinear saturated absorption spectroscopy is a spectral hole-burning technique, widely used for Doppler-free spectroscopy [13,14], which has been evolving with the comb technology for multiplexed precision spectroscopy [15], and with nanophotonics for, e.g.,

* Corresponding authors at: State Key Laboratory of Precision Spectroscopy, East China Normal University, Shanghai 200062, China
E-mail addresses: myan@lps.ecnu.edu.cn (M. Yan), hpzeng@phy.ecnu.edu.cn (H. Zeng).

https://doi.org/10.1016/j.pacs.2022.100403
Received 7 July 2022; Received in revised form 20 September 2022; Accepted 20 September 2022
Available online 21 September 2022

bio-sensing with super spectral resolutions [16]. However, the hole-burning phenomenon in the gas phase only becomes significant as the homogeneous pressure collision broadening effect is far less prominent than Doppler broadening. This requires considerably low sample pressure, unfavorable for transmitting (through a collision-induced ro-vibrational to translational relaxation) and detecting the sound [17].

A powerful solution for improving PA detection, as also pointed out in reference [4], is quartz-enhanced PAS (QEPAS), a technique relying on acoustic resonance with a low-cost quartz tuning fork (QTF) [18,19]. As an acoustic quadrupole, a QTF has excellent environmental noise immunity and, as a mechanical damped oscillator, its resonance rises with reduced pressure (due to less energy loss). Also, because of the high Q-factor of a QTF (e.g., ~10^5), QEPAS can be extremely sensitive to gas concentrations (typically at the parts-per-billion or ppb level) [20], even without optical enhancement (restraining excitation wavelengths). The ultra-narrow QTF resonance bandwidth (less than a few Hz), however, limits the spectral acquisition predominantly in the way of frequency sweeping [18–21]. Comb-enabled multiplexed QEPAS, allowing for frequency self-calibrated simultaneous measurements of absorption lineshapes for accurate molecular fingerprinting, is missing. Besides, mid-infrared DCS [6,22], accessing strong fundamental molecular transitions, is promising, and its integration with a QTF for sensitivity enhancement is even more intriguing [23,24], but has yet to be verified. Furthermore, sub-Doppler nonlinear saturated QEPAS is undeveloped, leaving an open space for exploration.

In this paper, we integrate linear and nonlinear dual-comb technology with QEPAS to address the above issues. We demonstrate for the first time saturation spectroscopy with the sharp QTF resonance enhancement, which may lead to new opportunities for PA gas sensing with a sub-Doppler resolution.

2. Theory

Our demonstration is built on the newly developed concept of dual-comb PAS [3,4] (Fig. 1(a)). A series of paired comb lines (each from a comb) at frequencies $f_n^{(i)}$ (the index i = 1, 2 denotes the two combs and n = 0, ± 1, ± 2,.,) is absorbed by the molecules, generating PA waves at the paired lines' beat frequencies $\Delta f_n = |f_n^{(1)} - f_n^{(2)}|$, in which way the absorption is encoded into the PA waves. A one-to-one correspondence between the acoustic frequencies (AF), Δf_n, and the optical frequencies (OF), $f_n^{(1)}$ ($\approx f_n^{(2)}$), is established, provided $\Delta f_n << f_n^{(1)}$.

The PA waves are detected simultaneously with a QTF. Generally, the QTF can be modeled as a damped oscillator [18]:

$$M\frac{d^2x(t)}{dt^2} + h\frac{dx(t)}{dt} + kx(t) = F(t) \quad (1)$$

where $x(t)$ represents the pressure wave induced displacement, h the acoustic losses, M the mass, and k the stiffness of the quartz resonator. With the dual-comb excitation, the driving force ($F(t)$) is given by the superimposed pressure waves, which is different from the conventional cases with single-wavelength excitation [18–21]. The solution of this equation may be understood in the Fourier-transformed AF domain as a sum of discrete frequency components, $x(f) = \sum A(\Delta f_n) \cdot Q(\Delta f_n)$, where the intensity of the nth PA wave $A(\Delta f_n) = P(f_n^{(1)}) \cdot \alpha(f_n^{(1)})$ is determined by the excitation power (P) and the molecular absorption coefficient (α). The QTF response function, $Q(f)$, typically has a Lorentz shape with the resonance frequency, f_Q, and the bandwidth, Δf_Q. The vibrational to translation relaxation effect is not considered, assuming the relaxation rate is fast enough ($>> f_Q$). Due to the piezoelectric effect, the QTF converts the displacement, $x(f)$, into an electrical signal $S(f)$. The signal at $f = f_Q$ may be expressed as [18]:

$$S \propto \frac{Q \bullet P \bullet \alpha}{f_Q}. \quad (2)$$

With Q~10^5 (depending on the sample gas and pressure), ultra-sensitive PA detection may be achieved.

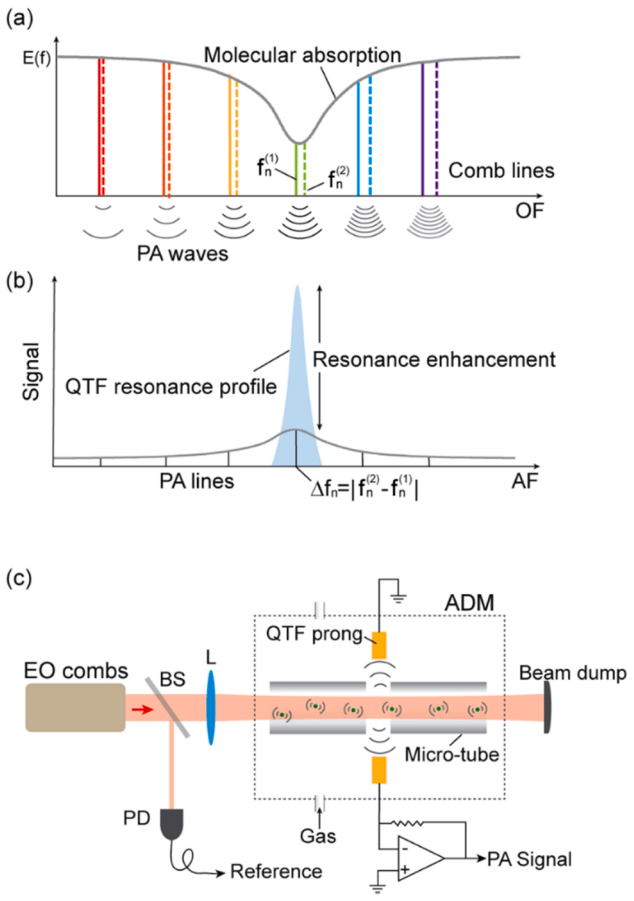

Fig. 1. Dual-comb quartz-enhanced photo-acoustic spectroscopy. (a) Photo-acoustic (PA) waves generated by molecules absorbing pairs of comb lines respectively from two optical combs. (b) The PA waves, whose frequency components (PA lines) form a third comb in the acoustic frequency (AF) domain, are detected by a quartz tuning folk (QTF). (c) Experimental setup. ADM, acoustic detection module; BS, beamsplitter; L, lens (f=100 mm); PD, photo-detector.

To measure the absorption lineshape (i.e., $\alpha(f)$), one must cram all the PA lines (as illustrated in Fig. 1(b)) into the sharp QTF resonance profile by reducing the difference between the line spacings of the two combs. For achieving the comb-line-defined resolution and precision, a measurement time of $t_m > N/\Delta f_Q$ is needed (N the total PA line number). The longer the measurement takes, the finer the resolved lines are, provided the combs' mutual coherence time $t_c \geq t_m$. A single measurement may take tens of seconds, for instance, to barely resolve a moderate number ($N = 100$) of PA lines for Δf_Q of a few Hz. This raises the challenge for the dual-comb coherence compared to using a microphone (typically with a bandwidth of several hundred Hz). Fortunately, the advancement in comb technology satisfies this demand [11]. For the sake of simplicity, we choose two mutually-coherent electro-optic (EO) combs for our proof-of-concept experiments.

3. Material and methods

The experimental setup is sketched in Fig. 1(c). A homemade dual EO comb generator and an off-the-shelf acoustic detection module (ADM) are utilized. Our approach to the EO combs is simple: a continuous-wave laser (frequency: f_{cw}) is split equally into two parts, each passing through an acoustic-optic modulator (driven frequency: $f_{aom}^{(i)}$~100 MHz) and subsequently an intensity modulator (modulation frequency: $f_r^{(i)}$). Consequently, two optical combs, each containing a set of comb lines at

$f_n^{(i)} = f_{cw} + f_{aom}^{(i)} + n \cdot f_r^{(i)}$ are generated. Apart from the simplicity, we emphasize the tunability and mutual coherence of the combs. The continuous-wave laser, constantly monitored by a wavemeter (WA-1650, Burleigh), is tunable from 186.21 to 197.23 THz (1520–1610 nm), a wide spectral range for sensing important hydrocarbons and carbon oxides, and the comb line-spacings, $f_r^{(i)}$, from 9 kHz to 1 GHz, satisfactory for high-resolution spectroscopy. The dual-comb relative coherence time exceeds 10 s. Combined with a 50:50 fiber coupler, the two combs are amplified with an erbium-doped fiber amplifier (EDFA) before being launched into the ADM (ADM01, Thorlabs) for gas sensing.

Inside the ADM, the combs are absorbed by the molecules, yielding PA waves at $\Delta f_n = \Delta f_{aom} + n \cdot \Delta f_r$, which resemble the third comb with a center at $\Delta f_{aom} = |f_{aom}^{(1)} - f_{aom}^{(2)}|$ and a line-spacing of $\Delta f_r = |f_r^{(1)} - f_r^{(2)}|$. All the waves are, ideally, in resonance with two micro-tubes placed on either side of a QTF (i.e., the on-beam configuration [18]). The effective acoustic coupling between the micro-tubes and QTF leads to a high-Q factor > 12000 at f_Q= 12467.8 Hz. The detection signal is amplified by an integrated pre-trans-impedance amplifier and then Fourier-transformed into a AF spectrum, which can be a posteriori calibrated on the OF axis, using a scaling factor, $f_r^{(1)}/\Delta f_r$, and a shift to the comb center frequency, $f_{cw} + f_{aom}^{(1)}$, where $\Delta f_r << f_r^{(1)}$ and $\Delta f_{aom} << f_{aom}^{(1)}$. For reference, a small portion (<5 %) of the dual-comb light, before entering the ADM, is detected by a photodetector. For spectral measurements, the PA signal and reference are digitized with a 16-bit acquisition card (ATS9626, AlazarTech) at a sample rate of 50 kHz. Besides, the radio-frequency signal generators for the EO combs and the digitizer are referenced to a hydrogen maser with frequency stability of 10^{-13} in 1 s. Also, the light beam is aligned properly (not touching the QTF prongs and the micro-tube walls) to minimize photothermal background. The setup is detailed in Supplement 1.

4. Results

4.1. Near-infrared measurements

Fig. 2(a) exemplifies the time-domain traces recorded with 2 % $^{12}C_2H_2$ (diluted in N_2) at room temperature (295 K) and one atmospheric pressure (~10^5 Pa). The gas volume is ~7 cm^3. The total light power inside the ADM is 3.5 mW. The PA signal is obtained by tuning f_{cw} to 195.895 THz (1530.37 nm), close to the P(9) ro-vibrational line of the overtone $\nu_1 + \nu_3$ band of $^{12}C_2H_2$, and by setting Δf_r = 0.5 Hz, $\Delta f_{aom} = f_Q$, and $f_r^{(1)}$ = 1 GHz. The comb parameters are set so that the PA lines lie within Δf_Q (<4 Hz at 10^5 Pa). In Fig. 2(a), the reference interferometric sequence is produced by the multi-heterodyne detection of the two combs (spectral width ~30 GHz). The PA trace differs from the reference because of optical bandwidth reduction since only the comb lines being absorbed (absorption bandwidth ~6 GHz) contribute to the PA signal. The comb-line-resolved PA spectrum is displayed in Fig. 2(b). The instrumental lineshape is imprinted on the PA lines (Fig. 2(b) inset), hence hardly affecting the absorption lineshape measurement.

A frequency-calibrated spectrum for another transition (the P(17) line) of the $\nu_1 + \nu_3$ band of 2 % $^{12}C_2H_2$ (in N_2) is shown in Fig. 3(a). For this measurement, the combs (f_{cw}=195.255 THz), with total power of 100 mW, are set near the transition frequency with adequate line-spacings ($f_r^{(1)}$ = 1 GHz, Δf_r = 0.25 Hz). The measurement takes 100 s. The spectrum (dark blue dots) in Fig. 3(a) is plotted using the PA line maxima normalized to a thermal background obtained with pure N_2 (i.e., the product of the dual-comb power spectrum and the QTF resonance profile). The spectrum represents five neighboring ro-vibrational transition lines of $^{12}C_2H_2$, whose assignments can be found in reference [25]. The line positions and their logarithmic linestrengths are schematically

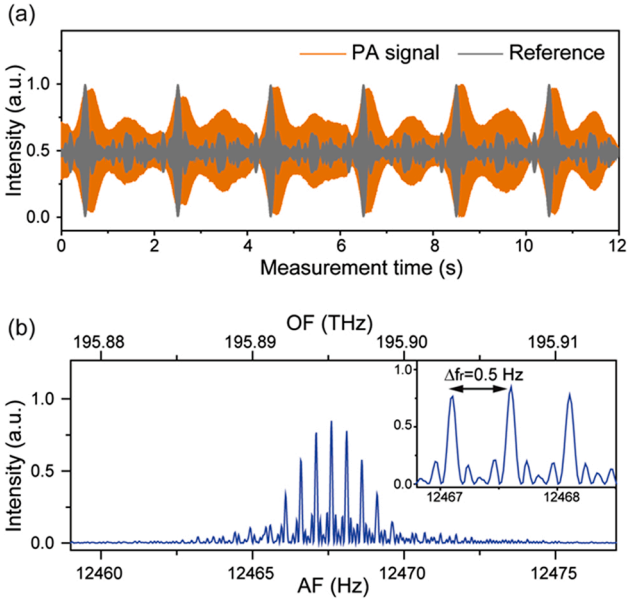

Fig. 2. Experimental results. (a) Recorded dual-comb traces for the PA signal and the reference. (b) Fourier-transform spectrum of the PA signal, displayed on both the AF and optical frequency (OF) axes. The spectrum corresponds to the $\nu_1 + \nu_3$ band P(9) line of $^{12}C_2H_2$. The enlarged dual-comb PA lines are shown in the inset. The AF resolution is 0.11 Hz for boxcar apodization.

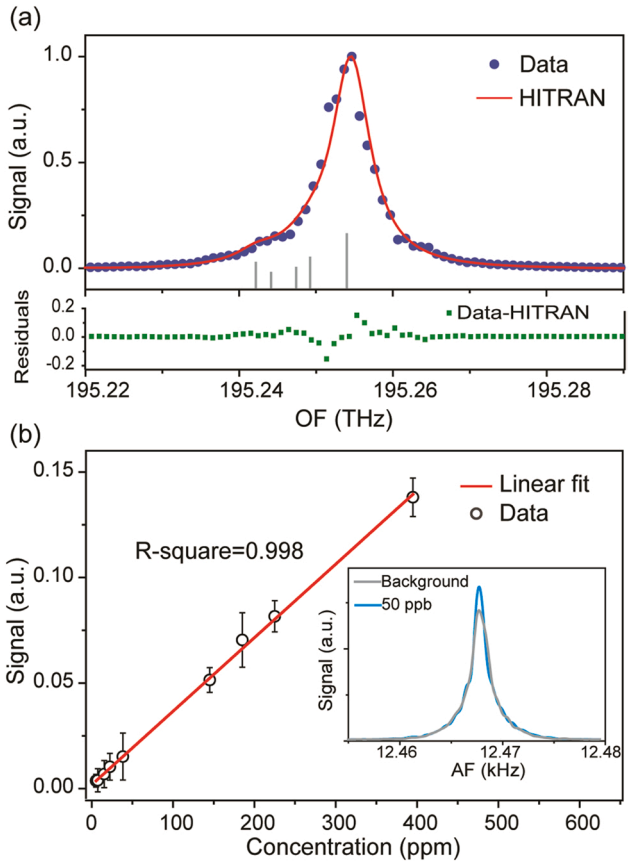

Fig. 3. Multiplexed dual-comb spectra with high sensitivity. (a) Normalized spectrum, showing multiple molecular transitions nearby the P(17) line of the $^{12}C_2H_2$ $\nu_1 + \nu_3$ band. The spectral resolution is set by the comb line-spacing of 1 GHz. The HITRAN simulation curve is superimposed on the experimental data. The residuals between the data and HITRAN are displayed in green. (b) Linear dependence of the PA spectral signal on $^{12}C_2H_2$ concentrations. The error bars are evaluated from ten separate measurements. The inset displays the spectrum for 50-ppb $^{12}C_2H_2$ (in N_2) and the thermal background.

depicted as the gray lines in Fig. 3(a), the strongest of which is the P(17) line (linestrength of 6.67 $\times 10^{-21}$ cm/molecule). A simulation curve (red), using the line parameters from the HITRAN database [26], is also displayed. Our experimental data agree well with the simulation within 3 %, quantified by the standard deviation of their residuals (solid green squares in Fig. 3(a)). The multiplexing capacity of DCS benefits QEPAS for simultaneously measuring molecular absorption lineshapes.

Fig. 3(b) plots the peak of the PA signal versus $^{12}C_2H_2$ concentrations. The linear fitting indicates excellent linearity with $R^2 = 0.998$. The inset displays an AF spectrum measured with 50-ppb $^{12}C_2H_2$ (for the P(17) line). The absorption lineshape is hardly distinguishable from the background (the gray curve) due to a limited signal-to-noise ratio (SNR). Subtracting the background from the signal (Fig. (b) inset), we estimate the SNR for the single-pass excitation to be ~6, which leads to a noise-equivalent concentration (NEC) of 8.3 ppb, three orders of magnitude lower than that of using a microphone (e.g., 10 ppm achieved for a similar linestrength within 1000 s) [4]. Notably, such sensitivity is obtained without optical enhancement (such as using optical cavities, hollow-core fibers, or multi-pass cells), making the system simple, robust, and easy to use. Also, the linear dynamic range, calculated by the ratio of the maximum non-saturation concentration (10^3 ppm) for a fixed dual-comb power ($P = 270$ mW) and the NEC, exceeds 10^5, which is mainly limited by the electronics and the digitizer. In the experiment, the minimum detectable absorption coefficient, α_{min}, is 4.13×10^{-9} cm^{-1}, calculated from the HITRAN database. For the number of spectral elements $N = \Delta f_Q/\Delta f_r$ (=16) and $t_m = 100$ s, the normalized noise equivalent absorption (NNEA) coefficient, defined as $P{\cdot}\alpha_{min}{\cdot}\sqrt{t_m/N}$, is 0.7×10^{-9} $cm^{-1}{\cdot}W{\cdot}Hz^{-1/2}$, a decent value comparing to that of frequency-swept QEPAS (e.g., ~10^{-9} $cm^{-1}{\cdot}W{\cdot}Hz^{-1/2}$ for acetylene gas [18]).

4.2. Mid-infrared spectra

It is of interest to implement our setup in the mid-infrared region, where sensitivity can be boosted with stronger absorptions and where sensitive photo-detection is challenging. To that end, we convert the near-infrared combs into the 3.3-μm (specifically 3.14–3.55 μm or 84.53–95.55 THz), using difference frequency generation (DFG) in a 10-mm-long periodically poled lithium niobate (PPLN) crystal pumped with a 1-W single-frequency laser emitting at 1064 nm (Fig. 4(a)). This approach for mid-infrared comb generation is well known [5,22], so we leave the detail to Supplement 1.

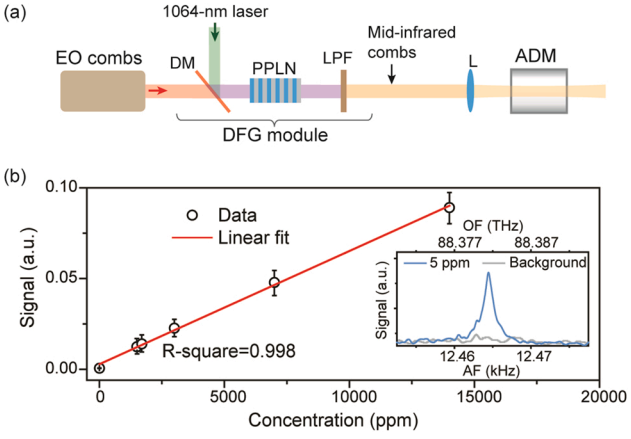

Fig. 4. Mid-infrared dual-comb experimental setup and results. (a) The EO combs, combining with a continuous-wave laser at 1064.01 nm (linewidth~10 kHz within 1 ms) on a diachronic mirror (DM), is launched into a 10-mm-long PPLN crystal, generating mid-infrared light around 3.3 μm via difference frequency generation (DFG). The mid-infrared light, spectrally filtered by a long-pass filter (cutoff at 2.4 μm), is then focused, with a BaF_2 lens (f=50 mm), into the ADM for spectral measurements. Inside the ADM is $^{12}CH_4$ mixed with N_2 at a total pressure of 10^5 Pa and temperature of 295 K. (b) The mid-infrared PA signal depends linearly on the $^{12}CH_4$ concentration. The inset displays the dual-comb PA spectrum of the sub-level $A_1^{(1)}$ line of the ν_3-band P(7) manifold for $^{12}CH_4$ of 5 ppm and a background measured with pure N_2.

For demonstration, the tetrahedral $A_1^{(1)}$ line of the ν_3-band P(7) manifold of $^{12}CH_4$ is measured, considering its relatively strong linestrength (8.41 $\times 10^{-20}$ cm/molecule). The other components in this manifold are isolated due to the limited detection bandwidth. Fig. 4(b) confirms the PA spectral peak linearly (R^2 =0.998) depending on the $^{12}CH_4$ concentration (diluted in N_2). The inset in Fig. 4(b) exemplifies a mid-infrared dual-comb PA spectrum (blue) for $^{12}CH_4$ of 5 ppm, measured with $\Delta f_r = 0.5$ Hz and $f_r^{(1)} = 0.5$ GHz, and a thermal background (gray) which is negligible due to the weak mid-infrared power (~0.08 mW). The SNR is 10, resulting in a NEC of 0.5 ppm. With $\alpha_{min} = 5.23 \times 10^{-6}$ cm^{-1}, we obtained a NNEA coefficient of 0.26×10^{-9} $cm^{-1}{\cdot}W{\cdot}Hz^{-1/2}$, which is reasonably lower (also better) than the near-infrared result.

4.3. Saturated QEPAS with dual-combs

Finally, we demonstrate saturation spectroscopy based on the pump-probe configuration (Fig. 5(a)). A high-power single-frequency pump laser saturates a transition for molecules in a specific velocity group, consequently causing hole burning (i.e., the Bennett hole, shown in black) on the Doppler-broadened absorption profile (gray curve). Conventionally, the hole, with a Doppler-free homogeneous lineshape, can be spectroscopically probed using a frequency-swept continuous-wave laser [13,14] or an optical comb [15]. Here, it is probed differently, using the dual-combs with PA detection. Gas pressure is vital for

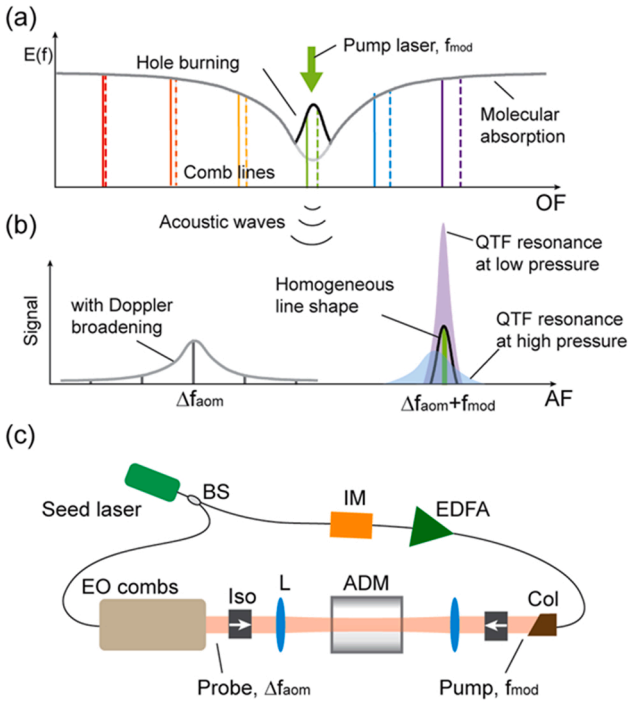

Fig. 5. Schematic diagram of saturated dual-comb QEPAS. (a) Spectral-hole burning with a strong pump laser. (b) The saturation signal with a homogeneous lineshape is separated from the Doppler background in the AF domain. The QTF resonance profile is sharpened and slightly shifted at low pressure (Supplement 1). The changes are considered in the measurement. (c) Experimental diagram. IM, intensity modulator; EDFA, erbium-doped fiber amplifier; Iso, optical isolator; Col, fiber collimator. The pump beam is a narrow-linewidth single-frequency laser (intensity modulated at f_{mod}) and the probe beam is the dual-combs. The beat frequency of the center lines of the two combs is Δf_{aom}, set by the two acoustic-optical modulators, each for an EO comb.

both the spectral hole-burning and PA detection. The hole can be sharpened and enhanced by reducing the pressure (narrowing the pressure-broadening linewidth), which, however, damps the sound waves. This difficulty may be alleviated by using a QTF with improved detection sensitivity due to the increased resonance at low gas pressure (because the acoustic losses of the oscillating QTF are reduced). Furthermore, for extracting the weak signal, the pump laser is intensity modulated at a small frequency, f_{mod} ($<f_Q$), and the center of the dual-comb beat notes (Δf_{aom}) is set as $\Delta f_{aom}+f_{mod}=f_Q$, so that the PA signals with and without Doppler broadening can be separated in the AF domain (Fig. 5(b)). Due to the narrow bandwidth of the QTF, only the saturation signal around f_Q (affected by both the pump and probe beams) can be recorded. Noises outside the bandwidth would be suppressed, hence benefiting the SNR. This strategy of intermodulation has long been used for weak signal detection in nonlinear spectroscopy [17] and works effectively in our case.

In this experiment, a narrow-linewidth continuous-wave laser (E15, NKT photonics; linewidth <1 kHz within 0.1 ms) is employed as a seed laser (Fig. 5(c)), whose output is split equally into two beams, one for seeding the EO combs and the other for the pump source. The pump laser is modulated at f_{mod} (=3 kHz, with a duty ratio of 50 %) via a fiber-coupled intensity modulator, subsequently amplified by an EDFA, and finally sent to the ADM from the opposite direction of the dual-comb port. Two free-space isolators are used to block the counter-propagating beams. The pump power in the ADM is 230 mW, and the combs 30 mW for 200 comb lines (i.e., 150 μW per comb line). See Supplement 1 for more details.

Fig. 6 exemplifies a Doppler-free spectrum for the $\nu_1+\nu_3$ band P(17) line of pure $^{12}C_2H_2$ at 200 Pa. The spectrum (dots) is measured at a comb-line-defined resolution of 10 MHz (i.e., $f_r^{(1)}=10$ MHz) within 200 s. We notice that the QTF bandwidth decreases to ~0.35 Hz at 200 Pa. As a countermeasure, Δf_r is further reduced to 0.02 Hz. Therefore, the effective OF bandwidth that we can measure is $0.35\cdot f_r^{(1)}/\Delta f_r$ Hz (=175 MHz). A Lorentz fit (red curve) of the data shows a homogeneous linewidth of 45.8 ± 1.0 MHz, within the allowed OF bandwidth. This saturation signal is evidenced by the fact that it disappears by blocking either of the counter-propagating beams and the fact that it is extremely sensitive to the pump laser frequency f_p ($=f_{cw}$). The signal is optimized by tuning f_{cw} to 195,254.543 GHz, when the hole burning occurs near the dual-comb spectral center ($f_{cw}+f_{aom}^{(1)}$) so as to be acoustically in resonance with the QTF. Note that the hole is pumped and probed at different optical frequencies, implying that the recorded line center (f_{pr}) deviates from the center of the P(17) transition, f_{P17}. Their relationship can be described as $f_{pr}=f_{P17}+(f_p-f_{P17})\cdot\boldsymbol{k}_p/\boldsymbol{k}_{pr}$, where $\boldsymbol{k}_p$ and $\boldsymbol{k}_{pr}$ are the wave vectors for the pump and the dual-comb probe beams respectively.

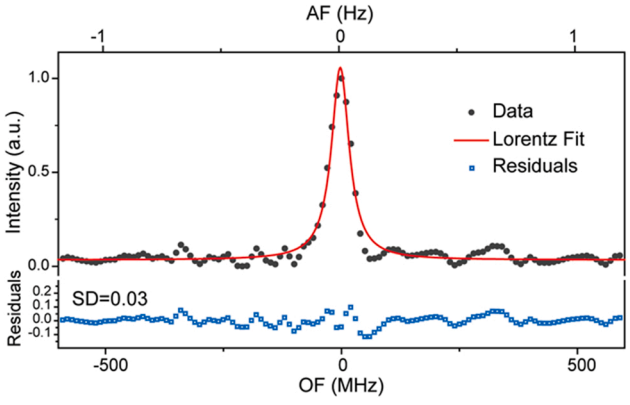

Fig. 6. Doppler-free spectrum measured with dual-comb QEPAS. The comb line maxima are plotted with dots. The comb-line-determined resolution is 10 MHz. The experimental profile, for the $^{12}C_2H_2$ $\nu_1+\nu_3$ band P(17) line, is fitted by a Lorentz function. The standard deviation of the residuals is 3 %. The offsets for the AF and OF axes are 12,467.8 Hz and 195,254.643 GHz, respectively.

For the collinear counter-propagating beams ($\boldsymbol{k}_p=-\boldsymbol{k}_{pr}$), the P17 line position is given by $f_{P17}=(f_{pr}+f_p)/2=(f_{pr}+f_{cw})/2$, where f_{pr} can be obtained from the fitting. The line position may be measured precisely, provided f_{cw} is calibrated to, e.g., a self-referenced frequency comb, rather than the wavemeter (an absolute accuracy >10 MHz) used in our experiment. Nevertheless, we emphasize on the high spectral resolution achieved here. The recorded homogeneous linewidth (45.8 MHz), an order of magnitude narrower than the Doppler-broadening limit (~470 MHz), manifests the feasibility of dual-comb QEPAS for sub-Doppler spectroscopic gas sensing.

There are also two things to note about this experiment. Firstly, the main contributors to the recorded linewidth include pressure broadening (18 MHz for 90 kHz/Pa) [27], transit-time broadening (~4 MHz) [28], and the frequency drift of the seed laser during the measurement (which is about ± 10 MHz measured by heterodyning with another continuous-wave laser). The frequency instability could be improved by stabilizing the seed laser against a self-referenced comb or an optical cavity. In such a case, further reducing the pressure would ideally lead to a narrower linewidth but would also cause problems. For instance, this would challenge the combs' mutual coherence due to the narrowing QTF resonance bandwidth. Also, the vibrational to transitional relaxation (depending on the gas species) would become too slow to match the QTF resonance frequency, hence disqualifying the PA detection. Accessing rotational transitions of the molecules with fast relaxation rates [18] (by using terahertz or far-infrared combs) and improving the dual-comb coherence with phase-control schemes [29] may alleviate these problems. Secondly, the optimized NEC we achieved with data averaging is 0.2 %. However, if necessary, the sensitivity could be further improved with optical resonance cavities [30] or multi-pass cavities [3] at the expense of increased system complexity.

5. Discussion

In most cases, QEPAS is performed with frequency-tunable lasers [31–36] (primarily quantum cascaded lasers for accessing the mid- and far- infrared or even THz regions). Compared to frequency-tunable QEPAS, there may be a few benefits of using dual-combs. For instance, it benefits optical frequency calibration. For our EO combs, the calibration can be performed simply by measuring the cw laser frequency. A commercial wavemeter will provide the accuracy required for most applications. Meanwhile, the signal generators set the comb line-spacings precisely, without taking further measures. It also renders instrumental lineshape effects negligible for comb-line resolved spectroscopic measurements.

On the other hand, a drawback of our scheme is the QTF bandwidth narrowing the single-shot spectral range, in which only a single molecular line or multiple neighboring lines are measured in a single measurement, and also limiting the acquisition speed. This drawback may be alleviated using QTF arrays [20]. Currently, this general issue of QEPAS limits our method to stationary measurements, but the method offers an exciting opportunity for QEPAS to work with optical combs [37]. The advances in frequency combs, respecting spectral coverages [10], pulse peak intensities [11], coherent times [29] and diverse platforms (e.g., portable fiber combs, on-chip microresonators [38], semiconductor lasers [39], etc.), may benefit QEPAS for precision measurements [40], for nonlinear spectroscopy, and for spectroscopic sensing at wavelengths where frequency-controlled lasers may not be available.

With the wavelength-independent acoustic sensor, our method is suitable for sensing a variety of gas species whose absorption lines are located within the combs' spectral range. Meanwhile, the sensitivity of the current setup is at the ppb level. However, we believe that with high-coherence (e.g., coherent time longer than 1000 s [29]) watt-level combs, and enhanced optical cavities (e.g., with 10^3-fold sensitivity enhancement [30]), our approach may lead to multiplexed spectral sensing at parts-per-trillion level or below.

Finally, regarding nonlinear spectroscopic measurements, we must mention that SA effects have been investigated for QEPAS [24,33–36]. For instance, gas sensing was performed for CO at SA conditions for theoretically and experimentally studying the impacts of SA effects on the overall performance of intra-cavity QEPAS [24]. A multilinear regression algorithm using the SA information of methane was also reported for properly evaluating gas concentrations for gas mixtures [34]. However, in most cases, optical saturation effects were avoided to maintain a linear relationship between the PA signal and gas concentrations [33–36]. To our knowledge, nonlinear SA spectroscopy has not been carried out with QEPAS. Since QEPAS has been demonstrated as an economical and powerful tool for gas sensing with a broad scope of applications, such as trace detection, environmental monitoring, breath diagnostics, and so on, it is of great interest to investigate its potential for nonlinear spectroscopy. For instance, measuring molecular absorption lines at sub-Doppler resolutions may improve the spectral specificity for, e.g., identifying isotopes with similar spectral signatures.

6. Conclusions

Here, we have explored multiplexed high-resolution QEPAS with optical frequency comb and dual-comb technology for the first time. Comb-line-resolved spectral measurements for $^{12}C_2H_2$ and $^{12}CH_4$ have been demonstrated in near- and mid-infrared regions, respectively. More importantly, saturated dual-comb QEPAS, enabling sub-Doppler spectroscopic measurements, could potentially improve the specificity for chemical sensing. Like other types of QEPAS, our method has merits, including wavelength-independent detection, high sensitivity (e.g., ~8.3 ppb for acetylene), small sample volume (~7 cm^3), and high practicality, which are important for gas sensing applications, including trace detection.

Declaration of Competing Interest

The authors declare that they have no known competing financial interests or personal relationships that could have appeared to influence the work reported in this paper.

Data Availability

The data that support the findings of this study are available from the corresponding author upon reasonable request.

Acknowledgements

This work was supported in part by the National Natural Science Foundation of China (grant numbers 12022411, 11621404, 61875243, and 62035005) and Shanghai Science and Technology Commission Project (grant number 2019SHZDZX01-ZX05).

Contributions

All authors contributed significantly to this work.

Appendix A. Supporting information

Supplementary data associated with this article can be found in the online version at doi:10.1016/j.pacs.2022.100403.

References

[1] J.M. Langridge, T. Laurila, R.S. Watt, R.L. Jones, C.F. Kaminski, J. Hult, Cavity enhanced absorption spectroscopy of multiple trace gas species using a supercontinuum radiation source, Opt. Express 16 (14) (2008) 10178–10188, https://doi.org/10.1364/OE.16.010178.

[2] B. Henderson, A. Khodabakhsh, M. Metsälä, I. Ventrillard, F.M. Schmidt, D. Romanini, G.A.D. Ritchie, S.T.L. Hekkert, R. Briot, T. Risby, N. Marczin, F.J. M. Harren, S.M. Cristescu, Laser spectroscopy for breath analysis: towards clinical implementation, Appl. Phys. B 124 (2018) 161, https://doi.org/10.1007/s00340-018-7030-x.

[3] J.T. Friedlein, E. Baumann, K.A. Briggman, G.M. Colacion, F.R. Giorgetta, A. M. Goldfain, D.I. Herman, E.V. Hoenig, J. Hwang, N.R. Newbury, E.F. Perez, C. S. Yung, I. Coddington, K.C. Cossel, Dual-comb photoacoustic spectroscopy, Nat. Commun. 11 (2020) 3152, https://doi.org/10.1038/s41467-020-16917-y.

[4] T. Wildi, T. Voumard, V. Brasch, G. Yilmaz, T. Herr, Photo-acoustic dual-frequency comb spectroscopy, Nat. Commun. 11 (2020) 4164, https://doi.org/10.1038/s41467-020-17908-9.

[5] I. Coddington, N. Newbury, W. Swann, Dual-comb spectroscopy, Optica 3 (4) (2016) 414–426, https://doi.org/10.1364/OPTICA.3.000414.

[6] N. Picqué, T.W. Hänsch, Frequency comb spectroscopy, Nat. Photon. 13 (3) (2019) 146–157, https://doi.org/10.1038/s41566-018-0347-5.

[7] P.-L. Luo, E.-C. Horng, Simultaneous determination of transient free radicals and reaction kinetics by high-resolution time-resolved dual-comb spectroscopy, Commun. Chem. 3 (2020) 95, https://doi.org/10.1038/s42004-020-00353-6.

[8] D.I. Herman, C. Weerasekara, L.C. Hutcherson, F.R. Giorgetta, K.C. Cossel, E. M. Waxman, G.M. Colacion, N.R. Newbury, S.M. Welch, B.D. DePaola, I. Coddington, E.A. Santos, B.R. Washburn, Precise multispecies agricultural gas flux determined using broadband open-path dual-comb spectroscopy, Sci. Adv. 7 (14) (2021) eabe9765, https://doi.org/10.1126/sciadv.abe9765.

[9] E. Vicentini, Z. Wang, K.V. Gasse, T.W. Hänsch, N. Picqué, Dual-comb hyperspectral digital holography, Nat. Photon. 15 (2021) 890–894, https://doi.org/10.1038/s41566-021-00892-x.

[10] T. Mizuno, E. Hase, T. Minamikawa, Y. Tokizane, R. Oe, H. Koresawa, H. Yamamoto, T. Yasui, Full-field fluorescence lifetime dual-comb microscopy using spectral mapping and frequency multiplexing of dual-comb optical beats, Sci. Adv. 7 (1) (2021) eabd2102, https://doi.org/10.1126/sciadv.abd2102.

[11] S.A. Diddams, K. Vahala, T. Udem, Optical frequency combs: coherently uniting the electromagnetic spectrum, Science 369 (6501) (2020) eaay3676, https://doi.org/10.1126/science.aay3676.

[12] A.S. Kowligy, H. Timmers, A.J. Lind, U. Elu, F.C. Cruz, P.G. Schunemann, J. Biegert, S.A. Diddams, Infrared electric field sampled frequency comb spectroscopy, Sci. Adv. 5 (6) (2019) eaaw8794, https://doi.org/10.1126/sciadv.aaw8794.

[13] G. Giusfredi, S. Bartalini, S. Borri, P. Cancio, I. Galli, D. Mazzotti, P.D. Natale, Saturated-absorption cavity ring-down spectroscopy, Phys. Rev. Lett. 104 (11) (2010), 110801, https://doi.org/10.1103/PhysRevLett.104.110801.

[14] A.K. Singh, L. Muanzuala, V. Natarajan, Precise measurement of hyperfine structure in the $2P_{1/2}$ state of ^{7}Li using saturated-absorption spectroscopy, Phys. Rev. A 82 (4) (2010), 042504, https://doi.org/10.1103/PhysRevA.82.042504.

[15] D.A. Long, A.J. Fleisher, D.F. Plusquellic, J.T. Hodges, Multiplexed sub-Doppler spectroscopy with an optical frequency comb, Phys. Rev. A 94 (6) (2016), 061801, https://doi.org/10.1103/PhysRevA.94.061801.

[16] V.P. Zharov, Ultrasharp nonlinear photothermal and photoacoustic resonances and holes beyond the spectral limit, Nat. Photon. 5 (2) (2011) 110–116, https://doi.org/10.1038/nphoton.2010.280.

[17] E.E. Marinero, M. Stuke, Doppler-free optoacoustic spectroscopy, Opt. Commun. 30 (3) (1979) 349–350, https://doi.org/10.1016/0030-4018(79)90368-7.

[18] P. Patimisco, G. Scamarcio, F.K. Tittel, V. Spagnolo, Quartz-enhanced photoacoustic spectroscopy: a review, Sensors 14 (4) (2014) 6165–6206, https://doi.org/10.3390/s140406165.

[19] H. Wu, L. Dong, H. Zheng, Y. Yu, W. Ma, L. Zhang, W. Yin, L. Xiao, S. Jia, F. K. Tittel, Beat frequency quartz-enhanced photoacoustic spectroscopy for fast and calibration-free continuous trace-gas monitoring, Nat. Commun. 8 (1) (2017) 15331, https://doi.org/10.1038/ncomms15331.

[20] P. Patimisco, A. Sampaolo, L. Dong, F.K. Tittel, V. Spagnolo, Recent advances in quartz enhanced photoacoustic sensing, Appl. Phys. Rev. 5 (2018), 011106, https://doi.org/10.1117/12.2284162.

[21] J.B. Christensen, L. Høgstedt, S.M.M. Friis, J.-Y. Lai, M.-H. Chou, D. Balslev-Harder, J.C. Petersen, M. Lassen, Intrinsic spectral resolution limitations of QEPAS sensors for fast and broad wavelength tuning, Sensors 20 (17) (2020) 4725, https://doi.org/10.3390/s20174725.

[22] M. Yan, P.-L. Luo, K. Iwakuni, G. Millot, T.W. Hänsch, N. Picqué, Mid-infrared dual-comb spectroscopy with electro-optic modulators, Light.: Sci. Appl. 6 (10) (2017), e17076, https://doi.org/10.1038/lsa.2017.76.

[23] J. Karhu, T. Tomberg, F.S. Vieira, G. Genoud, V. Hänninen, M. Vainio, M. Metsälä, T. Hieta, S. Bell, L. Halonen, Broadband photoacoustic spectroscopy of $^{14}CH_4$ with a high-power mid-infrared optical frequency comb, Opt. Lett. 44 (5) (2019) 1142–1145, https://doi.org/10.1364/OL.44.001142.

[24] J. Hayden, B. Baumgartner, J.P. Waclawek, B. Lendl, Mid-infrared sensing of CO at saturated absorption conditions using intracavity quartz-enhanced photoacoustic spectroscopy, Appl. Phys. B 125 (9) (2019) 159, https://doi.org/10.1007/s00340-019-7260-6.

[25] Q. Kou, G. Guelachvili, M.A. Temsamani, M. Herman, The absorption spectrum of C_2H_2 around $\nu1+\nu3$: energy standards in the 1.5 μm region and vibrational clustering, Can. J. Phys. 72 (11) (1994) 1241–1250, https://doi.org/10.1139/p94-160.

[26] I.E. Gordon, L.S. Rothman, R.J. Hargreaves, R. Hashemi, E.V. Karlovets, F. M. Skinner, E.K. Conway, C. Hill, R.V. Kochanov, Y. Tan, P. Wcisło, A.A. Finenko, K. Nelson, P.F. Bernath, M. Birk, V. Boudon, A. Campargue, K.V. Chance, A. Coustenis, B.J. Drouin, J. Flaud, R.R. Gamache, J.T. Hodges, D. Jacquemart, E. J. Mlawer, A.V. Nikitin, V.I. Perevalov, M. Rotger, J. Tennyson, G.C. Toon, H. Tran, V.G. Tyuterev, E.M. Adkins, A. Baker, A. Barbe, E. Canè, A.G. Császár, A. Dudaryonok, O. Egorov, A.J. Fleisher, H. Fleurbaey, A. Foltynowicz,

T. Furtenbacher, J.J. Harrison, J. Hartmann, V. Horneman, X. Huang, T. Karman, J. Karns, S. Kassi, I. Kleiner, V. Kofman, F. Kwabia–Tchana, N.N. Lavrentieva, T. J. Lee, D.A. Long, A.A. Lukashevskaya, O.M. Lyulin, V. Makhnev, W. Matt, S. T. Massie, M. Melosso, S.N. Mikhailenko, D. Mondelain, H. Müller, O. V. Naumenko, A. Perrin, O.L. Polyansky, E. Raddaoui, P.L. Raston, Z.D. Reed, M. Rey, C. Richard, R. Tóbiás, I. Sadiek, D.W. Schwenke, E. Starikova, K. Sung, F. Tamassia, S.A. Tashkun, J. Vander Auwera, I.A. Vasilenko, A.A. Vigasin, G. L. Villanueva, B. Vispoel, G. Wagner, A. Yachmenev, S.N. Yurchenko, The HITRAN2020 molecular spectroscopic database, J. Quant. Spectrosc. Radiat. Transf. 277 (2013), 107949, https://doi.org/10.1016/j.jqsrt.2021.107949.

[27] W.C. Swann, S.L. Gilbert, Pressure-induced shift and broadening of 1510–1540-nm acetylene wavelength calibration lines, J. Opt. Soc. Am. B 17 (7) (2000) 1263–1270, https://doi.org/10.1364/JOSAB.17.001263.

[28] J. Henningsen, J. Hald, J.C. Petersen, Saturated absorption in acetylene and hydrogen cyanide in hollow-core photonic bandgap fibers, Opt. Express 13 (26) (2005) 10475–10482, https://doi.org/10.1364/OPEX.13.010475.

[29] Z. Chen, M. Yan, T.W. Hänsch, N. Picqué, A phase-stable dual-comb interferometer, Nat. Commun. 9 (1) (2018) 3035, https://doi.org/10.1038/s41467-018-05509-6.

[30] Z. Wang, Q. Wang, H. Zhang, S. Borri, I. Galli, A. Sampaolo, P. Patimisco, V. L. Spagnolo, P.D. Natale, W. Ren, Doubly resonant sub-ppt photoacoustic gas detection with eight decades dynamic range, Photoacoustics 27 (2022), 100381, https://doi.org/10.1016/j.pacs.2022.100387.

[31] Y. Ma, W. Feng, S. Qiao, Z. Zhao, S. Gao, Y.Y. Wang, "Hollow-core anti-resonant fiber based light-induced thermoelastic spectroscopy for gas sensing,", Opt. Express 30 (2022) 18836–18844, https://doi.org/10.1364/OE.460134.

[32] Y. Ma, R. Lewicki, M. Razeghi, F.K. Tittel, "QEPAS based ppb-level detection of CO and N2O using a high power CW DFB-QCL,", Opt. Express 21 (2013) 1008–1019, https://doi.org/10.1364/OE.21.001008.

[33] V. Spagnolo, P. Patimisco, S. Borri, G. Scamarcio, B.E. Bernacki, J. Kriesel, Mid-infrared fiber-coupled QCL-QEPAS sensor, Appl. Phys. B 112 (2013) 25–33, https://doi.org/10.1007/s00340-013-5388-3.

[34] P. Luo, J. Harrist, G. Menduni, R. Mesdour, N. StMichel, A. Sampaolo, Simultaneous detection of methane, ethane, and propane by QEPAS sensors for on-site hydrocarbon characterization and production monitoring, ACS Omega 7 (2022) 3395–3406, https://doi.org/10.1021/acsomega.1c05645.

[35] S. Palzer, Photoacoustic-based gas sensing: a review, Sensors 20 (9) (2020) 2745, https://doi.org/10.3390/s20092745.

[36] H. Wu, L. Dong, X. Liu, H. Zheng, X. Yin, W. Ma, L. Zhang, W. Yin, S. Jia, Fiber-amplifier-enhanced QEPAS sensor for simultaneous trace gas detection of NH3 and H2S, Sensors 15 (10) (2015) 26743–26755, https://doi.org/10.3390/s151026743.

[37] I. Sadiek, T. Mikkonen, M. Vainio, J. Toivonen, A. Foltynowicz, Optical frequency comb photoacoustic spectroscopy, Phys. Chem. Chem. Phys. 20 (44) (2018) 27849–27855, https://doi.org/10.1039/C8CP05666H.

[38] A. Dutt, C. Joshi, X. Ji, J. Cardenas, Y. Okawachi, K. Luke, A.L. Gaeta, M. Lipson, On-chip dual-comb source for spectroscopy, Sci. Adv. 4 (3) (2018), e1701858, https://doi.org/10.1126/sciadv.1701858.

[39] S.M. Link, D.J.H.C. Maas, D. Waldburger, U. Keller, Dual-comb spectroscopy of water vapor with a free-running semiconductor disk laser, Science 356 (6343) (2017) 1164–1168, https://doi.org/10.1126/science.aam7424.

[40] T.W. Hänsch, Nobel lecture: passion for precision, Rev. Mod. Phys. 78 (2006) 1297–1309, https://doi.org/10.1103/RevModPhys.78.1297.

Dr. Xinyi Ren is a postdoctoral researcher at East China Normal University (Shanghai, China). She received her B.S. degree in Optoelectronic Information Science and Engineering from Nanjing University of Posts and Telecommunications and a Ph.D. degree in Optics from East China Normal University in 2022. She now focuses on the development photoacoustic spectroscopy with optical frequency combs.

Dr. Ming Yan received a B.S. in Electronics Engineering (2007) and a Ph. D degree in Optics (2012) at East China Normal University (Shanghai, China). He was a postdoc researcher at Max-Planck Institute of Quantum Optics (Garching Germany, 2013–2017), and then joined the State Key Laboratory of Precision Spectroscopy, ECNU in 2017. He is now a full professor with research interests including fiber lasers, optical frequency combs and molecular spectroscopy.

Zhaoyang Wen is a graduate student at East China Normal University (Shanghai, China). He received his B.S. degree from the physics department of East China Normal University in 2020. He now focuses on the development of mid-infrared lasers and frequency comb spectroscopy.

Hui Ma is a graduate student at East China Normal University (Shanghai, China). She received his B.S. degree from Yantai University in 2020. She now focuses on the development of electro-optic frequency combs.

Ran Li is a graduate student at East China Normal University (Shanghai, China). He received his B.S. degree from China University of Mining and Technology in 2020. He now focuses on precision measurements with optical frequency combs.

Dr. Kun Huang received PhDs from École Normale Supérieure de Paris (Paris, France) and East China Normal University (Shanghai, China) in 2015, then did post-doc in Pierre-and-Marie-Curie University. He joined the faculty of Shanghai Key Laboratory of Modern Optical System, University of Shanghai for Science and Technology in 2017 as a professor, and then joined the ECNU in 2019. He has authored or coauthored more than 70 academic papers in peer-reviewed journals. His current research interests include mid-infrared generation and detection.

Prof. Heping Zeng received the B.S. degree in physics from Peking University (Beijing, China) in 1990 and the Ph.D. degree from the Shanghai Institute of Optics and Fine Mechanics, Chinese Academy of Science, Shanghai, China, in 1995. He joined the faculty of State Key Laboratory of Precision Spectroscopy, East China Normal University in 1999 as a professor. His research interests include ultrafast photonics, Terahertz optics, optical frequency combs and single-photon optics. So far, he has published more than 250 papers in peer-reviewed journals including Phys. Rev. Lett., Laser Photonics Rev., Appl. Phys. Lett., Opt. Lett. Phys., Rev. A, Opt. Express and so on.